

# Low dimensional chaos in cardiac tissue

Dante R. Chialvo, Robert F. Gilmour Jr\* & Jose Jalife

Department of Pharmacology, SUNY Health Science Center,  
766 Irving Avenue, Syracuse, New York 13210, USA

\* Department of Physiology, New York State College of Veterinary  
Medicine, Cornell University, Ithaca, New York 14853-6401, USA

CHAOS is a term used to characterize aperiodic activity arising in a dynamical system, or in a set of equations describing the system's temporal evolution as a result of a deterministic mechanism that has sensitive dependence on initial conditions<sup>1</sup>. Chaos, in that sense, has been proposed to make an important contribution to normal and abnormal cardiac rhythms<sup>2-6</sup>. To date, however, descriptions of chaos in heart tissue have been limited primarily to periodically forced cardiac pacemakers<sup>2,6</sup>. Because many cardiac rhythm disturbances, particularly those initiated or perpetuated by re-entrant excitation, originate from within non-pacemaker cardiac tissues<sup>7-9</sup>, demonstrations of chaos in non-pacemaker tissue might provide a deterministic explanation for a wide variety of complex dysrhythmias. Here we report experimental evidence for chaotic patterns of activation and action potential characteristics in externally driven, non-spontaneously active Purkinje fibres and ventricular muscle. The results indicate that there is an apparent link between the mechanism of low dimensional chaos and the occurrence of reflected responses which could lead to more spatially disorganized phenomena. A detailed mechanism for the low dimensional chaos observed experimentally is pursued using a difference equation model. Critical features of the model include a non-monotonic relationship between recovery time during rhythmic stimulation and the state of membrane properties, and a steeply sloped recovery of membrane properties over certain ranges of recovery times. Besides explaining our results, the analytical model may pertain to irregular dynamics in other excitable systems, particularly the intact dysrhythmic heart.

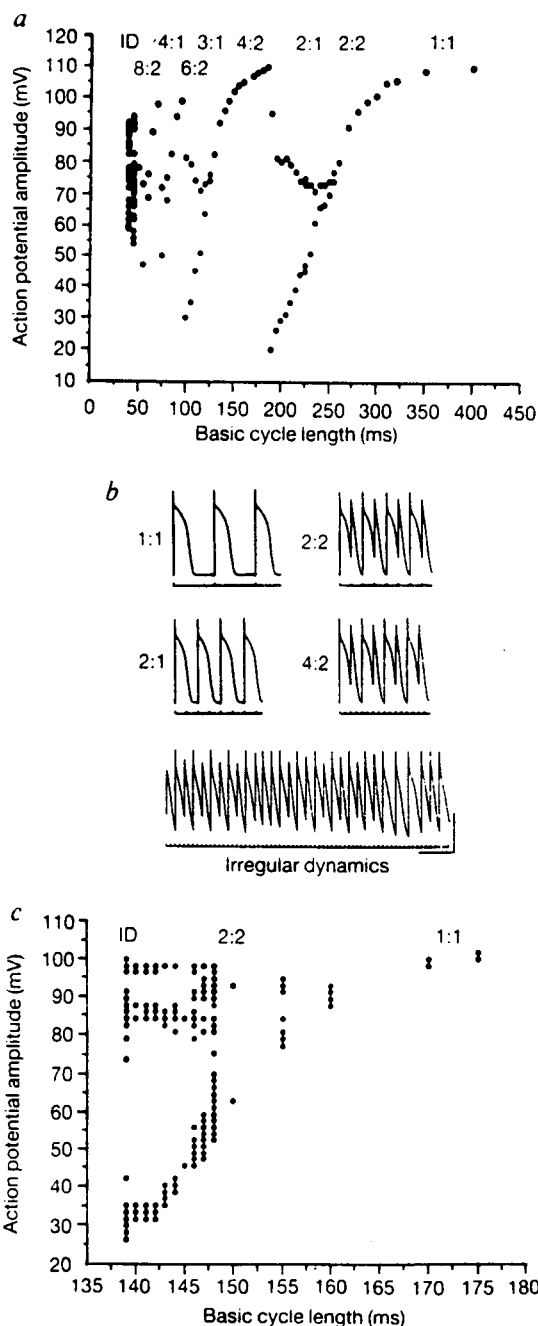
Chaos has been demonstrated in several experimental and theoretical models of periodically forced oscillators, including cardiac pacemakers<sup>1,2,6</sup>. Although non-autoactive excitable media may also display chaotic dynamics<sup>10</sup>, aperiodic responses of forced non-pacemaker cardiac tissue have been observed only under restricted experimental conditions<sup>11,12</sup>, which include low amplitude of stimulation in conjunction with supernormality.

FIG. 1 Period-doubling bifurcations and chaotic patterns of action potential amplitude in cardiac Purkinje fibres. *a*, Bifurcation diagram showing the relationship between pacing basic cycle length and beat-to-beat action potential amplitudes in a sheep cardiac Purkinje fibre. Stimulus: response locking indicated at top (ID, irregular dynamics). Stimulus intensity,  $1.5 \times$  threshold; KCl concentration, 2.7 mM. *b*, Analog recording of bifurcations and irregular dynamics obtained in a dog cardiac Purkinje fibre. Upper trace is transmembrane action potential and lower trace is stimulus record 1:1, 2:2, 2:1 and 4:2 locking were recorded at basic cycle lengths (BCLs) of 500, 145, 140 and 75 ms, respectively. Irregular dynamics preceding 3:1 locking were detected at BCL of 53 ms. Stimulus intensity,  $2.0 \times$  threshold; KCl concentration, 2.7 mM; calibration bars are 50 mV and 500 ms. *c*, Cascade of period doubling bifurcations, starting at 1:1 locking, leading to irregular dynamics in a sheep cardiac Purkinje fibre. Stimulus intensity,  $2.6 \times$  threshold; KCl concentration, 4.0 mM.

METHODS. Free running false tendons were obtained from the left ventricles of adult sheep ( $n=13$ ) following electrocution or from adult dogs ( $n=14$ ) following anaesthesia using pentobarbital sodium ( $35 \text{ mg kg}^{-1}$  intravenously). The preparations were mounted in a tissue bath and superfused with normal Tyrode solution maintained at pH 7.4,  $PO_2 > 400 \text{ mm Hg}$  and  $T=37.0^\circ\text{C}$ . The composition of the Tyrode solution (in mM) was:  $MgCl_2$  0.5,  $NaH_2PO_4$  0.9,  $CaCl_2$  2.0,  $NaCl$  137.0,  $NaHCO_3$  24.0,  $KCl$  2.7 or 4.0 and glucose 5.5. A concentration of 2.7 mM was used for KCl in some experiments to enhance supernormality<sup>11,22</sup>. Transmembrane recordings were obtained using floating glass microelectrodes, as described previously<sup>12,27</sup>. Pacing stimuli were 2.0 ms duration rectangular pulses obtained from a pulse generator and delivered through an isolation transformer at variable intensities.

Further studies of a simple experimentally based mathematical model<sup>12</sup> indicate that chaos might be a more general phenomenon associated with particular modes of nonlinear, time-dependent recovery of critical membrane properties in excitable tissues. Specifically, chaotic dynamics are predicted under experimental circumstances in which either significant delay to activation at very early recovery intervals, or non-monotonic recovery of action potential duration occurs. These theoretical predictions are explored here by a systematic examination of aperiodic behaviour in non-spontaneously active cardiac Purkinje fibres and ventricular muscle.

To demonstrate low dimensional chaotic behaviour in cardiac tissue, we initially determined whether a cascade of period-doubling bifurcations leading to more irregular activity occurred during decremental pacing. Figure 1*a* illustrates initial period doubling bifurcations of action potential amplitude occurring in a cardiac Purkinje fibre paced at increasing frequencies (that is, at decreasing cycle lengths). Period-doubling bifurcations



were associated with changes in stimulus:response locking, in that 1:1 locking was replaced by 2:2, 2:1 by 4:2, 3:1 by 6:2, and 4:1 by 8:2, until irregular activity arose at very brief cycle lengths. Careful exploration of the transition between 4:2 and 3:1 revealed that irregular dynamics also occurred at intermediate pacing rates. An example of such a transition is shown in Fig. 1*b*. The results shown in Fig. 1*a* and *b* provide experimental evidence for the theoretical predictions made previously<sup>12</sup>.

In Fig. 1*c*, stimulus amplitude is higher than that used in Fig. 1*a* and *b*. As the basic cycle length was abbreviated, a 2:2 locking pattern was followed by an additional period-doubling bifurcation (that is, 4:4) and then by irregular dynamics. The structure of the bifurcation diagram is similar to that observed during the period doubling route to chaos in unidimensional maps<sup>13-16</sup>. We sought additional experimental evidence to demonstrate conclusively that this irregular activity was in fact deterministic chaos. A return map of irregular sequences of action potential amplitude is depicted in Fig. 2. Successive data points are confined to specific regions of the return map, rather than being distributed randomly, indicating an underlying one-dimensional deterministic mechanism. Moreover, the data are distributed along two segments: a long descending segment that intersects the identity line (that is,  $APA_{n+1} = APA_n$ , where APA is the action potential amplitude) and a shorter ascending segment. Both the slope of the descending segment (less than minus one) and the order of appearance of consecutive data in the map (Fig. 2*b*) indicate a sensitive dependence on initial conditions and, therefore, a deterministic (chaotic) origin of the irregular activity<sup>12-20</sup>.

A simple theoretical model originally introduced by Guevara *et al.*<sup>18</sup> and further modified by us<sup>12</sup> can account for these experimental observations. As summarized in Fig. 3*a*, the main arguments used in the model are: (1) the recovery of relevant membrane properties after each action potential is nonlinear and (2) the fixed time between pulses during rhythmic stimulation generates reciprocal interactions between the recovery time (represented in the model by diastolic interval) and the degree of recovery of membrane properties (latency and action potential

duration). In such a feedback loop, there is a particular range of pacing cycle lengths within which period-doubling bifurcation and chaos are expected.

Figure 3*b* shows the predicted bifurcation sequence for experiments similar to those illustrated in Figs 1*c* and 2. In both experimental and theoretical cases, chaos always occurred after at least one period-doubling bifurcation. Likewise, the experimental and theoretically derived return maps during chaos (Figs 2 and 3*c*, respectively) were similar. It is apparent from the analytical model that the slope of the descending segment of the map is determined by the time constant of the fast component of the time to full repolarization function in Fig. 3*a* for a diastolic interval between -100 and 0 ms), whereas the ascending branch reflects prolongation of the time to full repolarization at short (that is, negative) diastolic intervals (Fig. 3*a*). Supernormal excitability<sup>23</sup> facilitates activation at short diastolic intervals, where recovery of action potential amplitude and time to full repolarization are non-monotonic ('notched') (Fig. 3*a*). As the rate of stimulation is increased, the slope of the map (Fig. 3*c*) at the intersection with the identity line becomes progressively steeper until it equals one, at which point a period-doubling bifurcation occurs. Additional increases in stimulus rate produce a cascade of period-doubling bifurcations and chaos. These observations reflect the known dynamical consequences for functions that contain both a steep slope and a minimum value<sup>13,24,25</sup>, so the existence of a minimum in the map guarantees that higher period doubling and chaos will occur.

In the absence of a minimum, represented here by the inflection point in the time to full repolarization versus diastolic interval function, 1:1 locking is replaced only by an initial period doubling bifurcation (2:2) (refs 18, 24) and then by 2:1 locking. This particular bifurcation scenario (presented in Fig. 1*a* and *b*) can be readily reproduced in the model by lowering stimulation amplitude so that the time to full repolarization function minimum disappears<sup>12</sup>.

Period-doubling bifurcations of action potential characteristics and chaotic patterns of activation were also demonstrated

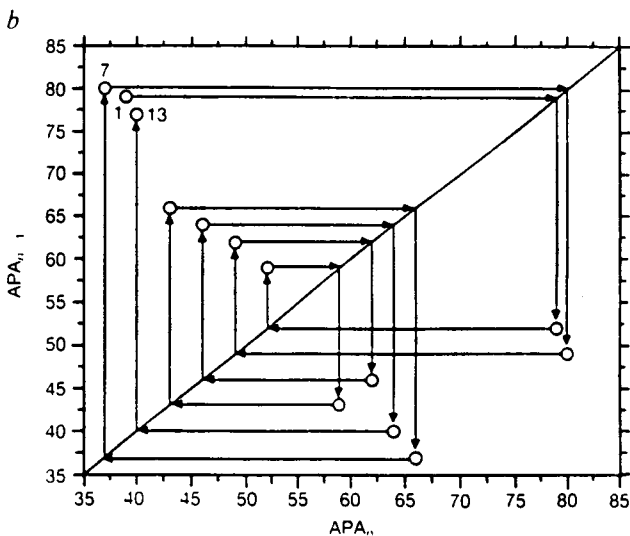
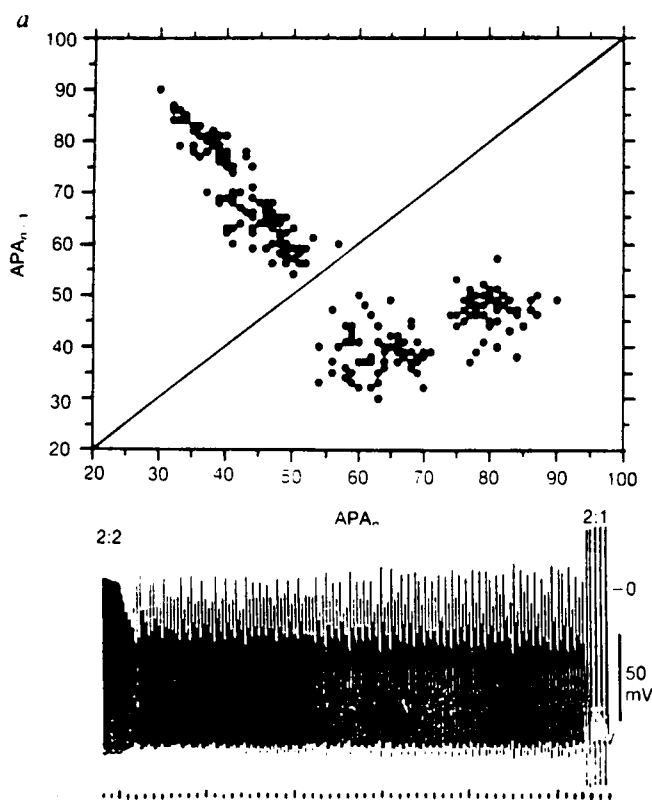
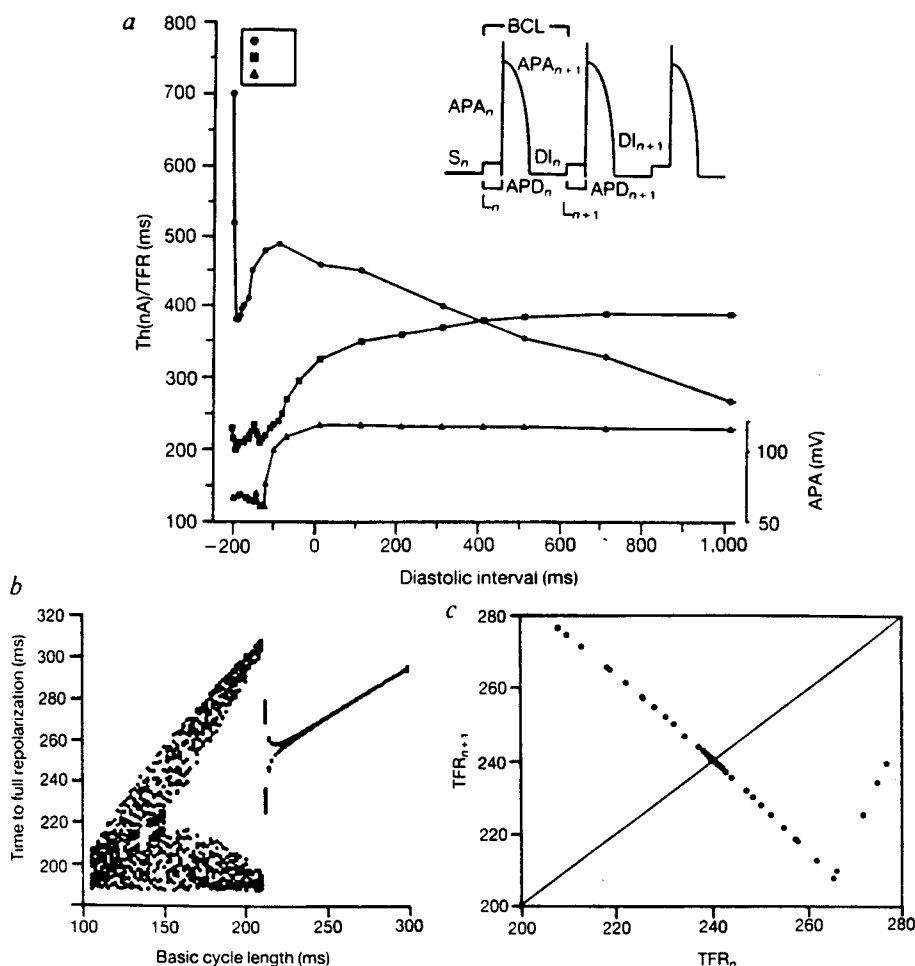


FIG. 2 Low dimensional chaos in a sheep cardiac Purkinje fibre. *a*, Lower record. Transmembrane recording obtained during pacing at a BCL of 180 ms. Brief records during pacing at BCL of 185 ms (2:2 locking, left) and 175 ms (2:1 locking, right) are also shown. Stimulus intensity,  $2.0 \times$  threshold; KCl concentration, 4.0 mM. Timescale is 1 s per division. Upper panel. Corresponding one-dimensional return map for APA, where  $APA_{n+1}$  is given for each preceding  $APA_n$ . For  $APA_n < 75$  mV,  $APA_n$  and  $APA_{n+1}$  are linearly related (slope, 1.441;  $r^2 = 0.891$ ). *b*, Return map of a portion of the irregular dynamics shown in *a*. Arrows indicate the sequence of the map, starting at 1 and ending at 13 (upper left). The fibre is different from that used in Fig. 1*c*. Methods are described in the legend to Fig. 1.

**FIG. 3** Period-doubling bifurcations and chaos in an analytical model of cardiac cells. *a*. Inset (upper right) shows the relevant parameters for the difference equation model. If latency to activation ( $L$ ), total action potential duration (APD), current threshold for all-or-none excitation ( $Th$ ) and action potential amplitude (APA) are functions ( $F$ ,  $G$ ,  $Z$  and  $Q$ , respectively) of the diastolic interval ( $DI$ ), where  $DI_n$  is  $BCL - L_n - APD_n$ ,  $S$  is stimulus and APA is the difference between the resting membrane potential and the peak voltage attained following a stimulus, then (1)  $L_{n+1} = F(DI_n)$ ; (2)  $APD_{n+1} = G(DI_n)$ ; (3)  $Th_{n+1} = Z(DI_n)$ ; and (4)  $APA_{n+1} = Q(DI_n)$ . No distinction has been made between active and passive membrane responses. Recovery of  $Th$  (circles), time to full repolarization (TFR, where  $TFR = L + APD$ ; squares), and APA (triangles) are given as functions of  $DI$ . Values were obtained experimentally from a sheep Purkinje fibre, as described previously<sup>27</sup>. For the simulation presented in *b* and *c*, model functions  $F$ ,  $G$  and  $Z$  were reconstructed by linear interpolation between data points. As measurements of  $L$  and APD during stimulation at high frequencies involve imprecise estimations of the completion of repolarization (see, for example, the analog records of irregular dynamics in Fig. 1*b*), APA was used to characterize the experimental dynamics. APA has a defined functional relationship with  $DI$  and, therefore, with TFR (see *a*). For presentation of the numerical results, TFR was chosen because it is the relevant parameter in the model. Note the supernormal phase of excitability (when  $Th$  is less than expected from a monotonic exponential decay) at  $DI$  of  $-180$  to  $-20$  ms. Note also non-monotonic behaviour of TFR and APA (notches) at  $DI$  between  $-200$  and  $-180$  ms and between  $-145$  and



$-105$  ms. *b*, Predicted bifurcation diagram showing the relationship between BCL and TFR for 60 iterations of the model at each BCL. *c*, Return map for TFR at a BCL of 150 ms.

in ventricular muscle cells of Purkinje-muscle preparations (Fig. 4). Rhythmic stimulation of the Purkinje fibre resulted in bifurcation behaviour in ventricular muscle cells (Fig. 4*a*) very similar to that observed in the Purkinje fibre preparation. Return maps of ventricular muscle responses reconstructed during periodic (period three in Fig. 4*b*) and aperiodic (Fig. 4*c*) activity indicate the existence of the same dynamical mechanism (steep slope and minimum) already described for Purkinje fibres. In ventricular muscle, as in the Purkinje fibres, the critical slope in the return map (Fig. 4*c*) is provided by the fast component of the action potential duration restitution function. The ascending segment of the map, reflecting significant conduction delays through Purkinje-muscle junctional cells following activation at short diastolic intervals, is associated with depressed conduction (induced by heptanol and hyperkalaemia<sup>26,27</sup>). Under these experimental conditions, the 'notches' in the time to full repolarization curve (Fig. 3*a*) are accentuated, thereby permitting the development of complex dynamics.

Whereas the chaotic dynamics in Purkinje fibres occurs in relatively homogeneous tissue (no spatial component), an important spatial parameter is present in the Purkinje-muscle preparations. A fascinating point is that both situations (essentially space-independent in Purkinje fibres, but space-dependent in Purkinje-muscle preparations) collapsed in a one-dimensional behaviour that is reproduced by a simple model.

For the reasons given, induction of chaotic activation at Purkinje-muscle junctions depends significantly on activation delay. As expected, prolonged activation delay also facilitates reflection<sup>27,28</sup> of impulses between ventricular muscle and the

Purkinje fibre and within ventricular muscle (Fig. 4*d*). Interestingly, both reflection and chaos occur over the same range of cycle lengths, whereas period two is commonly observed in the absence of reflected responses. Further studies (in progress) may clarify whether 'overlap' of the requirements for chaos and reflection could explain the experimental observations of period two, but not chaos, preceding more (spatially) disorganized activity such as ventricular fibrillation<sup>29</sup>.

The mechanism we propose for low dimensional chaos in non-pacemaker cardiac cells incorporates general properties common to other nonlinear dynamical systems, ranging from lasers to electronic devices<sup>30</sup>. Our studies indicate that pharmacological manipulations directed towards the steeply sloped and minimum functions of the model may prevent chaos. Accordingly, drugs that linearize the restitution of action potential amplitude and duration, prevent premature activation and its associated activation delays, or minimize activation delay directly, may suppress the development of cardiac dysrhythmias<sup>32,31,32</sup>. □

Received 31 July; accepted 14 December 1989.

- Glass, L., Shrier, A. & Belair, J. in *Chaos* (ed. Holden, A.) 237-256 (Princeton University Press, 1986).
- Guevara, M. R., Glass, L. & Shrier, A. *Science* **214**, 1350-1353 (1981).
- Smith, J. M. & Cohen, R. J. *Proc. natn. Acad. Sci. U.S.A.* **81**, 233-237 (1984).
- Glass, L., Goldberger, A. L., Courtremanche, M. & Shrier, A. *Proc. R. Soc. A* **413**, 9-26 (1987).
- Goldberger, A. L. & Rigney, D. R. in *Dynamic Patterns in Complex Systems* (eds Kelso, J. A. S., Schlesinger, M. F. & Mandell, A. J.) 248-264 (World Scientific, Singapore, 1988).
- Glass, L., Guevara, M. R., Shrier, A. & Perez, R. *Physica* **7D**, 89-101 (1983).
- El-Sherif, N., Mehra, R., Gough, W. B. & Zeiler, R. H. *Circ. Res.* **51**, 152-166 (1982).
- Kramer, J. B., Saffitz, J. E., Witkowski, F. X. & Corr, P. B. *Circ. Res.* **66**, 736-754 (1985).

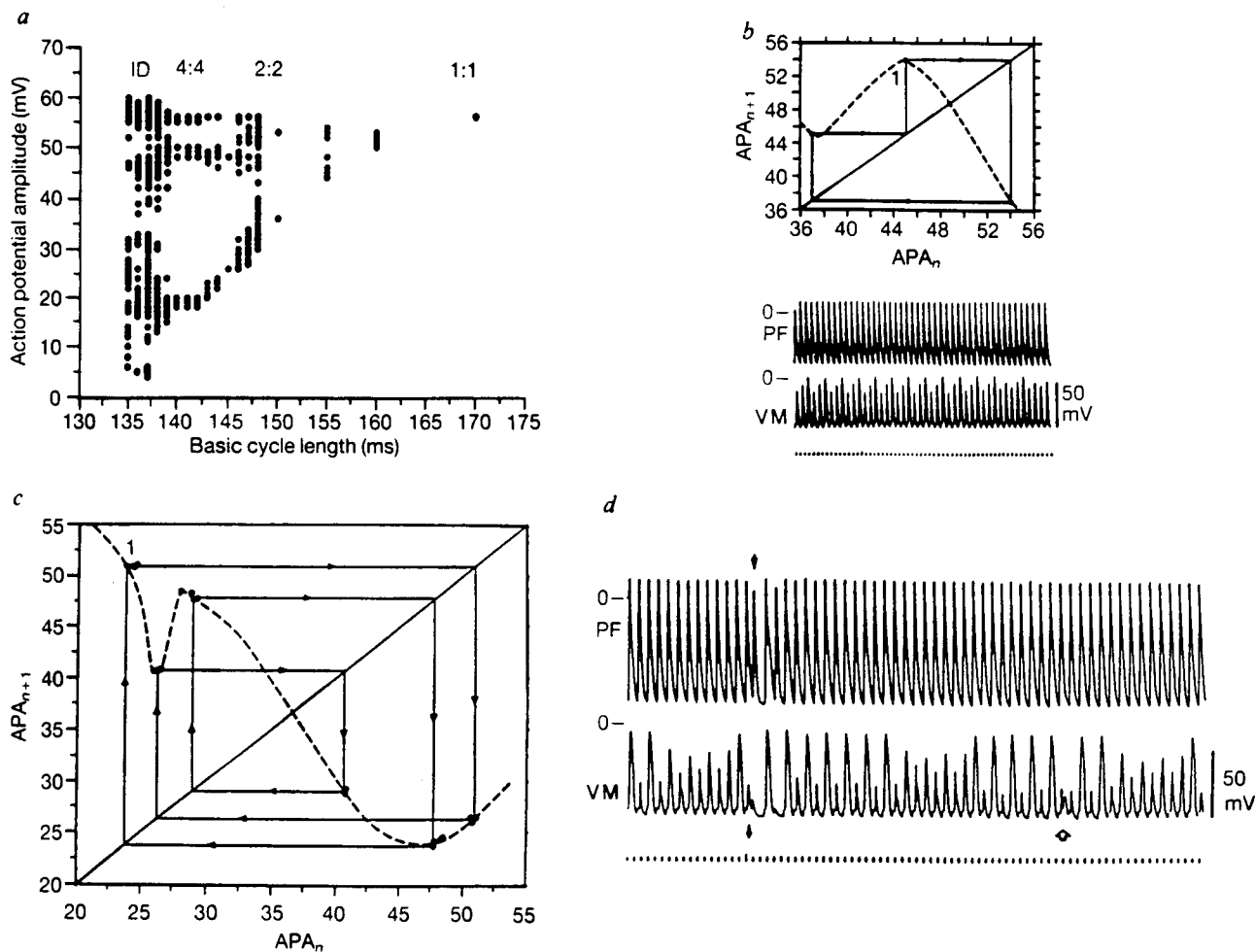


FIG. 4 Period-doubling bifurcations and chaos in canine Purkinje-muscle preparations. *a*, Bifurcation diagram showing beat-to-beat ventricular muscle action potential amplitude at different pacing cycle lengths. Similar results were obtained in five other preparations. *b*, Lower record, Transmembrane recordings of period 3 in ventricular muscle (VM; lower trace) during pacing of Purkinje fibre (PF; upper trace) as a BCL of 135 ms. Timescale 100 ms per division. Upper record, Corresponding return map for VM APA. *c*, Return map for aperiodic VM APA at a BCL of 147 ms. Four consecutive sequences are shown, starting at 1 (upper left). When all data were considered ( $n=62$ ), the slope of the regression line connecting points 1, 4, 5 and 6 was  $-1.243$ ,  $r^2=0.979$ . *d*, Transmembrane recordings during chaotic activity obtained from a Purkinje cell (upper trace) and a ventricular muscle cell (lower trace) during constant pacing of the Purkinje fibre at a BCL of 137 ms. During chaos conduction from PF to VM was accompanied by foot potentials and

by marked activation delays preceding short-duration VM action potentials. Following a critical activation delay, the VM action potential caused retrograde re-excitation of PF, which in turn, caused a second activation of VM, so that reflection of activation occurred between PF and VM (filled arrow). Reflection also seemed to occur within VM (inferred from biphasic VM action potential; unfilled arrow). Timescale is 100 ms per division.

**METHODS.** Hearts were removed from adult mongrel dogs of either sex following anaesthesia using pentobarbital sodium ( $35 \text{ mg kg}^{-1}$ ). Preparations ( $n=8$ ) of free-running false tendons attached to a 2–3 wide crescent of papillary muscle were excised from the left ventricle and mounted in a tissue bath, as described previously<sup>27</sup>. Pacing stimuli were delivered to the Purkinje fibre. Following equilibration in normal Tyrode solution, the preparation was superfused with Tyrode solution containing 6.0 mM KCl and 0.5 mM heptanol. Other methods described in the legend to Fig. 1.

9. Janse, M. J. in *The Heart and Cardiovascular System* (eds Fozzard, H. A. et al.) 1203–1238 (Raven, New York, 1986).  
 10. Matsumoto, G. et al. *Phys. Lett.* **A123**, 162–166 (1987).  
 11. Chialvo, D. R. & Jalife, J. *Nature* **330**, 749–752 (1987).  
 12. Chialvo, D. R. & Jalife, J. in *Cardiac Electrophysiology: From Cell to Bedside* (eds Zipes, D. P. & Jalife, J.) (Saunders, Philadelphia, in the press).  
 13. May, R. M. *Nature* **261**, 459–467 (1976).  
 14. Feigenbaum, M. J. *J. stat. Phys.* **19**, 25–52 (1978).  
 15. Lindsay, P. S. *Phys. Rev. Lett.* **47**, 1349–1352 (1981).  
 16. Simoyi, R. H., Wolf, A. & Swinney, H. L. *Phys. Rev. Lett.* **49**, 245–248 (1982).  
 17. Keener, J. P. *J. math. Biol.* **12**, 215–225 (1981).  
 18. Guevara, M. R., Ward, G., Shrier, A. & Glass, L. in *Computers in Cardiology 167–170* (IEEE Computer Soc., Long Beach, California, 1984).  
 19. Guevara, M. R., Shrier, A. & Glass, L. *Am. J. Physiol.* **254**, H1–H10 (1988).  
 20. Shaw, R. *The Dripping Faucet as a Model Chaotic System* 1–113 (Aerial, Santa Cruz, 1984).  
 21. Elharrar, V. & Surawicz, B., *Am. J. Physiol.* **244**, H782–H792 (1983).  
 22. Boyett, M. R. & Jewell, B. R. *Prog. Biophys. molec. Biol.* **36**, 1–52 (1980).

23. Spear, J. F. & Moore, E. N. *Circ. Res.* **35**, 782–792 (1974).  
 24. Glass, L. & Mackey, M. *From Clocks to Chaos. The Rhythms of Life* 1–248 (Princeton University Press, 1988).  
 25. Berge, P., Pomeau, Y. & Vidal, C. in *Order Within Chaos. Towards a Deterministic Approach to Turbulence* 1–329 (Wiley, New York, 1984).  
 26. Gilmour, R. F., Jr in *Cardiac Electrophysiology: From Cell to Bedside* (eds Zipes, D. P. & Jalife, J.) (Saunders, Philadelphia, in the press).  
 27. Gilmour, R. F., Jr, Davis, J. R. & Zipes, D. P. *Circulation* **76**, 1388–1396 (1987).  
 28. Antzelevitch, C., Jalife, J. & Moe, G. K. *Circulation* **61**, 182–191 (1980).  
 29. Ritzberg, A., Adam, D. & Cohen, R. *Nature* **307**, 159–161 (1984).  
 30. Moon, F. C. *Chaotic Vibrations. An Introduction for Applied Scientists and Engineers* 1–309 (Wiley, New York, 1987).  
 31. Varro, A., Elharrar, V. & Surawicz, B. *J. Pharmacol. Exp. Ther.* **233**, 304–311 (1985).  
 32. Colatsky, T. J. & Hogan, P. M. *Circ. Res.* **46**, 543–552 (1980).

**ACKNOWLEDGEMENTS.** We thank D. C. Michaels and M. Guevara for discussion and M. Buddie and W. Coombs for assisting with some of the experiments. These studies were supported by the NIH.